Pis'ma v ZhETF, vol. 101, iss. 11, pp. 869 – 872 © 2015 June 10

Excitation wave propagation in a patterned multi-domain cardiac tissue

N. N. Kudryashova, A. S. Teplenin, Y. V. Orlova+, K. I. Agladze[1)]

Laboratory of Biophysics of Excitable Systems, Moscow Institute of Physics and Technology, 141701 Dolgoprudny, Russia

+*iCeMS Research Building, Yoshida Honmachi, Sakyoku, Kyoto 606-8501, Japan*

Submitted 24 March 2015
Resubmitted 23 April 2015

Electrospun fibrous mats are widely used in the contemporary cardiac tissue engineering as the substrates for growing cardiac cells. The substrate with chaotically oriented nanofibers leads to the growth of cardiac tissue with randomly oriented, but internally morphologically anisotropic clusters or domains. The domain structure affects the stability of the excitation propagation and we studied the stability of the propagating excitation waves versus the average size of the domains and the externally applied excitation rate. In an experimental model based on neonatal rat cardiac tissue monolayers, as well as in the computer simulations we found that increase of domain sizes leads to the decrease of the critical stimulation frequencies, thus evidencing that larger domains are having a higher arrhythmogenic effect.

DOI: 10.7868/S0370274X15110107

1. Introduction. Electrospun fibrous mats are widely used in the contemporary cardiac tissue engineering [1–3]. They make versatile and handy scaffolds for the growing cultured tissue with relatively easy control of the tissue architecture [4]. However, a deep understanding of the correlation between the cardiac patch's morphology and its functional properties is required in order to avoid a dangerous mismatch of the created implant and the host tissue. For example, it is now recognized that the border between areas with different cell alignment may have a profound arrhythmogenic effect [5]. From the other hand, the electrospun fibrous mats made from the randomly applied polymer nanofibers often give rise to the patterned, multi-domain cardiac tissue, in which within each small domain the cells are essentially aligned, while the direction of the alignment sharply changes in the neighboring domains [4].

In the present work we analyzed the propagation of excitation in the multi-domain excitable medium both computationally and in the in vitro model of cardiac tissue. We studied the stability of the propagating excitation waves versus the average size of the domains and the externally applied excitation rate. As an experimental model we used neonatal rat cardiac tissue monolayers grown on the flat substrates covered with the oriented in random directions electrospun nanofibers [4].

As described earlier the single nanofiber leads to the elongation of cardiomyocytes situated in its proximity in the fiber direction [4, 6, 7]. The substrate with chaotically oriented nanofibers leads to the growth of cardiac tissue with randomly oriented, but internally morphologically anisotropic clusters or domains. Varying the positioning density of nanofibrous scaffold we achieved morphologically patterned cardiac monolayers with different average size of domains. Then we applied external electrical stimulation with different frequencies to the tissue layers with various clusters scales and observed their functioning with the aid of the optical mapping [8]. We determined highest (critical) frequency at which one-to-one response to external stimuli occurs for each type of cultures with different domain size. After optical mapping experiments all samples were actin stained, the exact sizes of the clusters were determined.

2. Experimental setup. In order to eliminate natural variations from sample to sample, the experimental system was designed in a way, shown in Fig. 1. Half of the glass cover slip was covered by the polymer nanofibers and another half was set free of fibers. Cells were seeded on the entire cover slip and cultured for 3–5 days. After that, electric stimulation was applied to the both parts of the cover slip with cultured tissue, as shown in Fig. 1. Since the cells and the conditions for culturing were identical for both halves of the glass substrate, the only difference in excitation propagation was due to the nanofibers defined architecture of the tissue versus fiber-free uniform distribution of the cultured cardiac cells. In order to avoid mutual interference of the wave patterns formed in the different parts of the

[1)]e-mail: agladze@yahoo.com

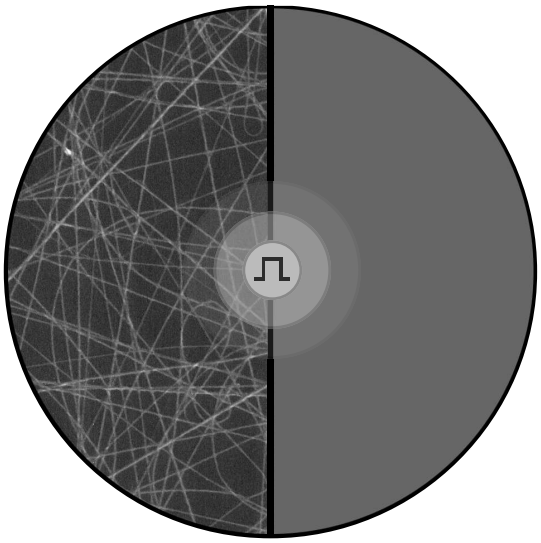

Fig. 1. Experimental setup. Right half of the glass cover slip was covered by randomized polymer nanofibers. Two halves were separated by thin cut and stimulation was applied at the edge between two parts. We have measured a critical frequency that captured only in fiber-free part

cell monolayer, immediately before the experiment they were separated by thin cut made along the border between two areas. Frequency of stimulation was raised from 1 to 10 Hz, until frequency is captured in fiber-free part, but propagation in fiber-covered part is broken.

3. Simulation. We consider two-variable Aliev–Panfilov model for simulation of excitation waves propagation in a cardiac tissue:

$$\dot{u} = \nabla[D(\mathbf{x})\nabla u] + cu(1-u)(u-a) - u,$$
$$\dot{v} = \left(\epsilon_0 + \frac{\mu_1 v}{\mu_2 + u}\right)[cu(1+a-u) - v],$$

where u is a membrane potential, v is a recovery variable, $D(\mathbf{x})$ is a coupling coefficients matrix that will be described precisely below, c is an excitability, a is an excitation threshold, and finally parameters μ_1, μ_2, and ϵ_0 are specific for this model and optimized for fitting the cardiac action potential [9]. This model was chosen for this study, because in spite of its simplicity, it accurately describes the trailing edge, which is quite important for simulation of wave series, stimulated with high frequency. Detailed ionic models [10–12] provide better approximation of action potential, but require more computational time, than two-variable models [13, 14].

4. Defining coupling coefficients. One of the most important parts of current computer modelling is the generation of a map of anisotropic clusters, that reproduces main feachures of the real clusterized cardiac monolayer, such as: cluster size, anisotropy ratio in clusters and average coupling in the sample. First, we made a triangulation of a 2D sample with periodic boundary conditions. Thus, the characteristic size of the triangle determines a characteristic size of the domain. Then, we assign some random preferential direction φ to each network node. Therefore, we determine coupling coefficients matrix in all vertices of a triangle as follows:

$$D = \begin{pmatrix} \lambda_1 \cos^2\varphi + \lambda_2 \sin^2\varphi & (\lambda_1 - \lambda_2)\sin\varphi\cos\varphi \\ (\lambda_1 - \lambda_2)\sin\varphi\cos\varphi & \lambda_1 \sin^2\varphi + \lambda_2 \cos^2\varphi \end{pmatrix},$$

where λ_1 and λ_2 are coupling coefficients along and across preferential direction.

Finally, we interpolate D within the triangle. Since two coefficients in D are equal, we can rewrite previous equation as

$$D = \begin{pmatrix} P & R \\ R & Q \end{pmatrix}$$

and interpolate diffusion tensor, assigning a triangle in geometric space to a triangle in (P, Q, R) space. As a result of this operation, centers of the triangles will become less anisotropic, than nodes and edges (Fig. 2). After adjustment the rule for selection of (P, Q, R) to fit distributions of λ_1 and λ_2 after interpolation (Fig. 3),

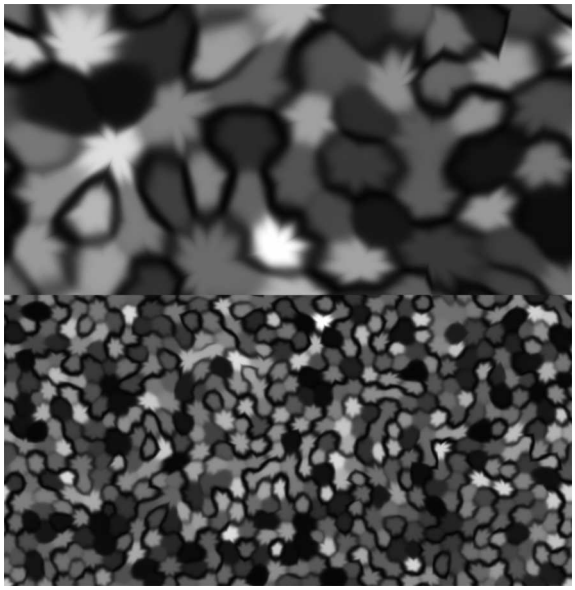

Fig. 2. Anisotropy ratio (λ_1/λ_2) map with periodic boundary for different domain sizes. These maps were generated in computational studies using algorithm described in Section 4. As far as the interpolation has been done in (P, Q, R) space, some clusters are divided with low anisotropy areas (black) and in some neighbouring clusters the preferential direction was just rotated, without significant anisotropy change

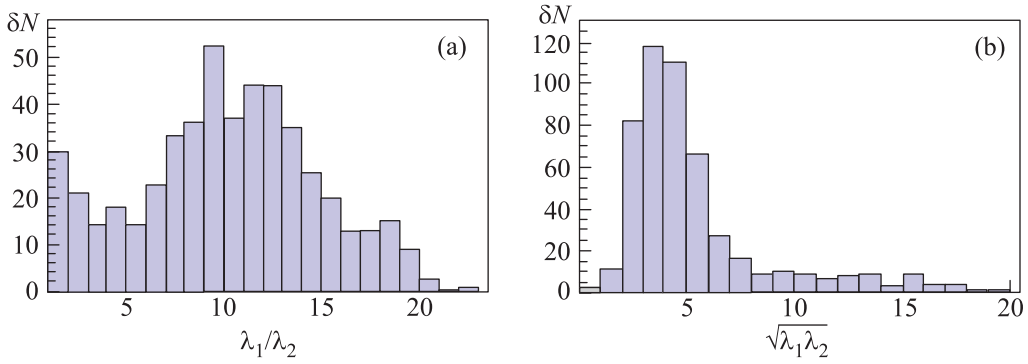

Fig. 3. Distributions of anisotropy ratio (λ_1/λ_2) (a) and average coupling ($\sqrt{\lambda_1\lambda_2}$) (b)

we obtain a model of an excitable media relevant to the cells, clusterized on the nanofibrous net.

4.1. Electrophysiological simulation. After establishing different maps of $D(\mathbf{x})$ with various domain sizes, controlled by triangulation, we can find the dependence of excitation waves behavior on the frequency of stimulation. We found that wave series demonstrate three different modes of propagation for the fixed domain size: a) the frequency is too high: not all stimuli can give a rise to a wave according to refractory zone of the previous one; b) waves are interacting by intersection with the refractory zone. Waves may break apart or even form spirals; c) the frequency is low. Waves are propagating almost independently, without any perturbations (Fig. 4).

5. Results. Applying different rates of stimulation we determined the maximal captured frequency in the fiber-covered and fiber-free parts of the sample. The frequency is captured, if every stimuli induces a travelling pulse. However, each wave leaves a refractory zone after passing through the media and the consequent wave could not enter this region, until the refractorness disappears. In solid media without domains and any inhomogeneities this interaction between the wave and previous refractory tail results in destruction of the wave and the frequency in a media becomes less than the frequency of stimulation. In a sample with domains this interaction becomes more complicated: the wave accelerates and decelerates travelling between the domains [5] and interacts with the refractory tail sooner or later; the refractory tail will also undergo some perturbations. As the result, we see some local blocks of propagation, resulting in wavebreaks.

The resulting graph is shown in Fig. 5. We tested the range of domains 5−200 μm and found that larger domain sizes lead to the decrease of the critical frequencies. Thus, these results show that cardiac patches of varying morphology can behave in a different way in

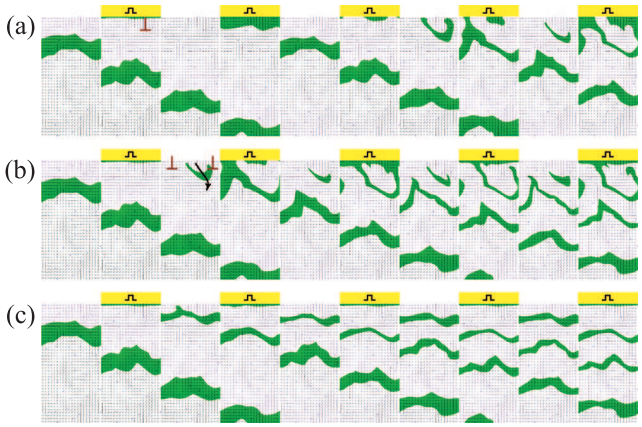

Fig. 4. Modes of excitation waves propagation with different stimulation frequencies. The depolarized regions, where $u \neq 0$, are shown in grey. Stimulation was applied at the top borders of the samples at the moments of time marked with square pulse sign. (a) – The frequency is too high: not all stimuli can give a rise to a wave according to refractory zone of the previous one. (b) – Waves are interacting by intersection with the refractory zone. Waves may break apart or even form spirals. (c) – The frequency is low. Waves are propagating almost independently, without any perturbations

the host patients myocardium in the response to different pacing rhythms and when exceeding critical rate could be the possible sources of arrhythmias.

We found the dependence of the critical frequency for wave-break formation on the size of the domains (Fig. 6). Hence, we observed in experiment two modes, found in simulation: b and c, and avoided mode a, when the stimulation is not captured.

We have shown, that if cell clusters are 20–50 times smaller, than the wavelength, then under high frequency of stimulation excitation waves could break apart and form spirals. If clusters are 19 times smaller, than the wavelength, or even larger, then normal propagation is

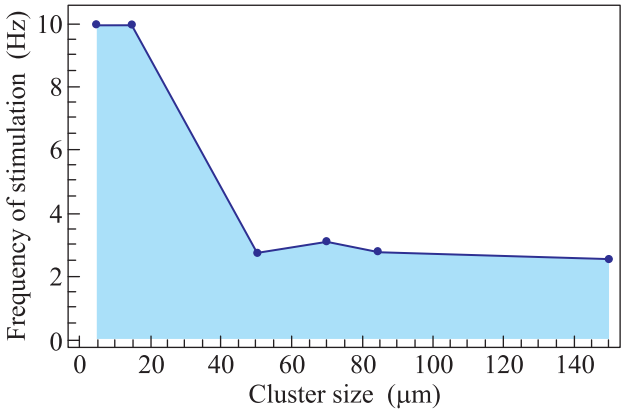

Fig. 5. Critical frequency of stimulation for various domain sizes, measured in experiment

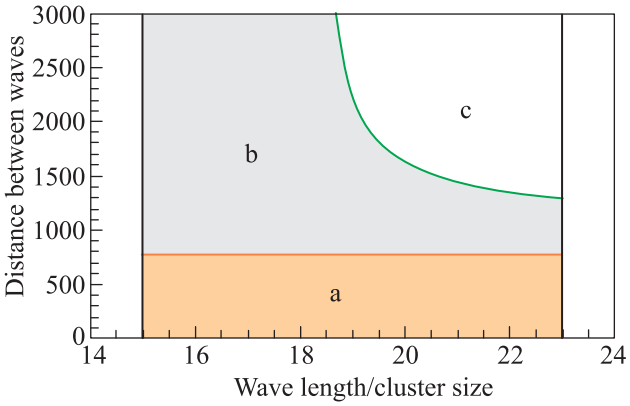

Fig. 6. Critical distance between waves in a series for various domain sizes, obtained from simulation

not even possible for a single excitation wave. However, clusters on nanofibrous nets are 60–1000 times smaller than the wavelength and for large clusters we have detected wave-breaks formation under high frequency of stimulation. We used two-variable Aliev–Panfilov model for excitation propagation simulation, that predicted the mode b (Fig. 4). However, the exact sizes of the domains and frequencies could be distinct from experimentally measured values.

The aim of our study was to exhibit the importance of the microstructure of engineered cardiac tissue, that could play arrhythmogenic role. Even if there are no macroscopic obstacles for wavebreak formation, a number of micro-domains with slightly different properties (e.g. preferential direction orientation) could also perturb the propagation of excitation and lead to reentry formation.

6. Conclusion. Our results show that in producing the scaffolds for the cardiac tissue engineering it is very important to control the architecture of the electrospun nanofibrous mats in order to achieve less arrhythmogenic cardiac implants. To avoid this, the density of the deposited fibers should be calculated from the features of the propagating excitation waves, so that the resulting cells domains will be smaller than the characteristic wavelength in the system.

The research was partially supported by Federal "5top100" Program.

1. S. Heydarkhan-Hagvall, K. Schenke-Layland, A. P. Dhanasopon, F. Rofail, H. Smith, B. M. Wu, R. Shemin, R. E. Beygui, and W. R. MacLellan, Biomaterials **29**(19), 2907e14 (2008).
2. M. Y. Li, Y. Guo, Y. Wei, A. G. MacDiarmid, and P. I. Lelkes, Biomaterials **27**(13), 2705e15 (2006).
3. J. L. Lowery, N. Datta, and G. C. Rutledge, Biomaterials **31**(3), 491e504 (2010).
4. Y. Orlova, N. Magome, L. Liu, Y. Chen, and K. Agladze, Biomaterials **32**(24), 5615 (2011).
5. N. N. Kudryashova, A. S. Teplenin, Y. V. Orlova, L. V. Selina, and K. Agladze, J. Mol. Cell. Cardiol. **76**, 227 (2014).
6. N. Bursac, Y. H. Loo, K. Leong, and L. Tung, Biochem. Bioph. Res. Co. **361**(4), 847 (2007).
7. N. Bursac, K. K. Parker, S. Iravanian, and L. Tung, Circ. Res. **91**(12), e45 (2002).
8. K. Agladze, M. W. Kay, V. Krinsky, and N. Sarvazyan, Am. J. Physiol-Heart C **293**, 503 (2007).
9. R. R. Aliev and A. V. Panfilov, Chaos Solit. Fract. **7**(3), 293 (1996).
10. C. H. Luo and Y. Rudy, Circ. Res. **68**, 1501 (1994).
11. C. H. Luo and Y. Rudy, Circ. Res. **74**(6), 1071 (1994).
12. F. Fenton and A. Karma, Chaos **8**(1), 20 (1998).
13. R. FitzHugh, Bull. Math. Biophy. **17**(4), 257 (1955).
14. J. Nagumo, S. Arimoto, and S. Yoshizawa, **117**, 2061 (1962).